AGU PUBLICATIONS

JGR

Journal of Geophysical Research: Space Physics

RESEARCH ARTICLE
10.1002/2015JA021257

Key Points:
- Introduction of model probability density functions
- Analysis of multiscale and small-scale histograms
- Conditional probability studies of magnetic fluctuations

Correspondence to:
Z. Vörös,
zoltan.voeroes@oeaw.ac.at

Citation:
Vörös, Z., M. Leitner, Y. Narita, G. Consolini, P. Kovács, A. Tóth, and J. Lichtenberger (2015), Probability density functions for the variable solar wind near the solar cycle minimum, *J. Geophys. Res. Space Physics*, *120*, 6152–6166, doi:10.1002/2015JA021257.

Received 26 MAR 2015
Accepted 18 JUL 2015
Accepted article online 30 JUL 2015
Published online 27 AUG 2015

Probability density functions for the variable solar wind near the solar cycle minimum

Z. Vörös[1,2], M. Leitner[3], Y. Narita[1], G. Consolini[4], P. Kovács[5], A. Tóth[6], and J. Lichtenberger[2,7]

[1]Space Research Institute, Austrian Academy of Sciences, Graz, Austria, [2]Department of Geophysics and Space Sciences, Eötvös University, Budapest, Hungary, [3]Institute of Physics, University of Graz, Graz, Austria, [4]INAF-Istituto di Astrofisica e Planetologia Spaziali, Roma, Italy, [5]Geological and Geophysical Institute of Hungary, Budapest, Hungary, [6]Faculty of Education, Constantine the Philosopher University in Nitra, Nitra, Slovak Republic, [7]Geodetic and Geophysical Institute, RCAES, Hungarian Academy of Sciences, Sopron, Hungary

Abstract Unconditional and conditional statistics are used for studying the histograms of magnetic field multiscale fluctuations in the solar wind near the solar cycle minimum in 2008. The unconditional statistics involves the magnetic data during the whole year in 2008. The conditional statistics involves the magnetic field time series split into concatenated subsets of data according to a threshold in dynamic pressure. The threshold separates fast-stream leading edge compressional and trailing edge uncompressional fluctuations. The histograms obtained from these data sets are associated with both multiscale (B) and small-scale (δB) magnetic fluctuations, the latter corresponding to time-delayed differences. It is shown here that, by keeping flexibility but avoiding the unnecessary redundancy in modeling, the histograms can be effectively described by a limited set of theoretical probability distribution functions (PDFs), such as the normal, lognormal, kappa, and log-kappa functions. In a statistical sense the model PDFs correspond to additive and multiplicative processes exhibiting correlations. It is demonstrated here that the skewed small-scale histograms inherent in turbulent cascades are better described by the skewed log-kappa than by the symmetric kappa model. Nevertheless, the observed skewness is rather small, resulting in potential difficulties of estimation of the third-order moments. This paper also investigates the dependence of the statistical convergence of PDF model parameters, goodness of fit, and skewness on the data sample size. It is shown that the minimum lengths of data intervals required for the robust estimation of parameters is scale, process, and model dependent.

1. Introduction

The solar wind is a complex plasma system in which structures, wavy fluctuations, and turbulence coexist over multiple scales. Since the Sun variably emits a mixture of fast and slow streams and transient ejecta, a single mechanism cannot fully reproduce the observed complexity in the solar wind. Some aspects of this complexity can be described statistically only. Despite the structural and dynamical complexity, field and plasma fluctuations exhibit well-defined scalings over specific frequency ranges in power spectral density (PSD) log-log plots. The low-frequency part of the spectrum is believed to reflect the statistics of large-scale structures and their interactions [*Burlaga and Goldstein*, 1984]. Below the time scale of a day the self-similar inertial range of magnetohydrodynamic (MHD) turbulence is set up, where dissipation is supposed to be negligible and energy cascades toward the small scales (large wave numbers or high frequencies) [*Bruno and Carbone*, 2013]. At characteristic proton and electron scales energy dissipation in collisionless plasmas takes place leading to nonadiabatic heating of the solar wind [*Alexandrova et al.*, 2013].

Turbulence represents a candidate process which explains the inertial range energy transfer supplying free energy for the kinetic-scale dissipation processes. The energy transfer rate ϵ in an MHD turbulent cascade can be calculated from the PSDs; however, these estimations are based on certain theoretical assumptions [*Smith et al.*, 2006; *Stawarz et al.*, 2009]. On the other hand, in hydrodynamics the rigorous Kolmogorov's 4/5 law [*Kolmogorov*, 1941] represents a way to estimate ϵ from third-order structure functions. Similarly to the 4/5 law in hydrodynamics, a rigorous third-order moment relation to calculate ϵ, the "MHD Yaglom's law," was obtained for incompressible MHD case by *Politano and Pouquet* [1998].

In terms of probability distribution functions (PDFs) nonzero third-order moments correspond to skewed PDFs. In hydrodynamic turbulence zero skewness or a nonskewed PDF indicates that the turbulent cascade is absent [*Davidson*, 2004]. Therefore, the determination of ϵ should preferably be based on the estimation of third-order moments associated with skewed PDFs. However, direct evidence about the (non)stationarity of third-order moments or equivalently about the (non)stationarity of the asymmetric shape of PDFs is still missing. In the solar wind the PDFs associated with turbulence are rather symmetric and it is difficult to estimate the skewness [*Podesta et al.*, 2009].

We will study the statistical properties of the multiscale fluctuations on the basis of 1 min total magnetic field measurements near the solar cycle minimum in 2008, when alternating fast and slow streams were present. The time resolution (1 min) and the length of the considered time interval (1 year) ensures that the one-point unfiltered measurements contain the whole spectrum of fluctuations from turbulent small scales to large scales of solar ejecta, occurring over solar rotations. In what follows we will refer to these measurements as multiscale observations having always in mind that the spectral power of multiscale processes is dominated by the large-scale fluctuations and turbulence.

The small-scale statistical properties of two-point magnetic fluctuations will be evaluated on the basis of time-delayed data at the time scale of $\tau = 10$ min. This is a time scale within the inertial range of turbulence in the solar wind. Parametric model PDFs will be used to fit the histograms obtained from the magnetic field data. The skewness (S) and the estimated parameters of model PDFs will be estimated separately for the multiscale and the small-scale magnetic fluctuations.

We note that the skewness S estimated from B is not straightforwardly associated with the turbulent energy transfer rate ϵ. The third-order moment relation for calculating ϵ in the solar wind contains the components of the Elsässer field (combined magnetic and velocity fluctuations [*Politano and Pouquet*, 1998]). Nevertheless, the MHD Yaglom's law, derived under the hypothesis of incompressibility, isotropy, homogeneity, and stationarity, represents a rough approximation only, which is expected to describe certain aspects of MHD turbulence in the highly variable solar wind [*Bruno and Carbone*, 2013]. Therefore, we believe that it makes sense to further investigate the statistical features of magnetic fluctuations alone, studying also the nonstationarity aspects of their dynamics.

According to *Burlaga and Viñas* [2004] large-scale magnetic fluctuations are observed over time scales from hours to approximately 1 year. This means that the observation of the large-scale statistics is possible only by considering unfiltered long time series containing a representative number of the large-scale structures. High-pass filtering of the data, for example, time-delayed differencing, enhances the fluctuations over the small scales. Although filtered long time series allow us to study the statistics of multiscale fluctuations, the effect of large-scale structures on turbulence is unknown or studied only sporadically [*Vörös et al.*, 2006]. We argue that conditional statistics applied for both unfiltered and filtered time series can reveal important aspects of multiscale interactions.

We are going to show that the multiscale and the small-scale PDFs corresponding to the magnetic fluctuations during the whole year in 2008 are different from the conditional PDFs associated with magnetic fluctuations in the leading (compressional) and in the trailing edges of high-speed streams. Nevertheless, a few basic types of model PDFs can explain the magnetic fluctuation statistics in the solar wind. These models correspond to additive and multiplicative statistical processes involving also nonzero correlations. We use four types of parametric PDFs, two symmetric distributions (normal and kappa) and two skewed distributions (lognormal and log-kappa). The basic mathematical features of normal and lognormal distributions were described long ago, and their mathematical treatment can be found in textbooks. The kappa distribution arises from nonextensive statistical mechanics describing out-of-equilibrium systems with long-range correlations [*Tsallis*, 1988; *Leubner*, 2002]. The log-kappa distribution was introduced recently by *Leitner et al.* [2009]. As it is shown here, the meaning of the model PDF parameters and of the nonzero skewness depends on the time scale and on the nature of physical processes under consideration. As a consequence, the required sample size for the robust estimation of statistical parameters also varies according to the statistical conditioning.

The organization of the paper is as follows. Section 2 introduces the model PDFs and the methodology of the estimation of statistical parameters. In section 3 unconditional and conditional statistics is introduced for both multiscale and small-scale magnetic fluctuations. The model PDF parameters and the skewness are estimated for progressively larger data sample sizes. Section 4 summarizes our results.

2. Probability Distribution Functions for Space Plasmas

We study magnetic field fluctuations over the time scales associated with multiscale structures and over the inertial range of scales associated with turbulent interactions. Our goal is to introduce a minimum number of model PDFs which can explain substantial parts of magnetic field variability in the solar wind. To this end we will use the normal and kappa PDFs and their logarithmic counterparts. The kappa PDFs which arise from nonextensive physics allow us to model magnetic field data exhibiting large deviations from the normal distribution. Although kappa functions are commonly used to model non-Maxwellian particle velocity distribution functions (VDFs), the underlying physics associated with nonextensive statistics over the MHD and kinetic scales is rather different. To avoid confusion, we will shortly describe the differences between particle VDFs and magnetic field PDFs.

2.1. Particle VDFs

Particle VDFs in the solar wind exhibit low-energy near-Maxwellian core and high-energy suprathermal tails described by kappa functions [*Vasyliūnas*, 1968; *Scudder*, 1992; *Leubner*, 2004]. Collisionless space plasmas are often out of thermal equilibrium, and suprathermal particles can be accelerated by a number of mechanisms [*Marsch*, 2006; *Pierrard and Lazar*, 2010; *Livadiotis*, 2015]. There exists a strong connection between the long-tail kappa distributions or κ indices (see below) and the nonextensive statistical mechanics representing a generalization of Boltzmann-Gibbs statistics for out-of-equilibrium particle systems exhibiting long-range correlations [*Tsallis*, 1988; *Leubner*, 2002]. It has been shown that the thermodynamic temperature T can be uniquely defined for the nonextensive out-of-equilibrium systems as well, through the variance of VDFs (mean kinetic energy) or equivalently through the connection of entropy with internal energy. [*Livadiotis and McComas*, 2010]. The κ index appears as an independent thermodynamic variable with a physical meaning of enhanced correlations (long-range interactions) or as a parameter corresponding to different stationary states in plasma systems with the same T and n (density) residing in a thermal nonequilibrium state [*Livadiotis and McComas*, 2013]. As a consequence, for the characterization of nonextensive plasmas described by kappa distributions, three independent parameters are needed, (n, T, κ). This can be regarded as a generalization of the polytropic law for out-of-equilibrium plasmas [*Livadiotis*, 2015].

2.2. PDFs for Field and Plasma Statistics

Examination of the field or particle statistics over the scales of MHD turbulence or even over larger scales implies that the real in situ data contain contributions from different physical processes, structures, or (non)mixing plasmas with nonunique combinations of parameters (n, T, κ). While the large-scale statistics can reflect important aspects of solar variability or locally generated processes in the solar wind, the variance of PDFs might not correspond to any well-defined plasma temperature. For example, turbulence with the same types of plasmas might be confined to flux tubes having characteristic sizes within the inertial range of turbulence [*Borovsky*, 2008]. Analyzing longer data intervals involving multiple flux tubes can change the turbulence statistics significantly [*Borovsky*, 2008]. The frequently observed twisted flux tubes can be more unstable against Kelvin-Helmholtz instability or reconnection than unstable flux tubes [*Zaqarashvili et al.*, 2014a, 2014b]. This can lead to abundant local generation of turbulence containing mixing plasmas and boundaries [*Vörös et al.*, 2014].

In situ observations of solar wind plasma clearly show that at kinetic levels the plasma significantly deviates from thermal equilibrium [*Marsch*, 2006]. The local generation of reconnection and turbulence indicates that the occurrence of multiscale dynamical interactions are manifestations of the nonequilibrium dissipative processes driven by the radial evolution and complicated relaxation of different types of physical components, such as the mostly uniform fast wind, the more filamentary structured wind, and the highly transient and variable-speed solar wind [*Marsch*, 2006]. Numerical simulations show that mesoscale coherent structures (e.g., flux tubes) in the turbulent solar wind can merge or repel each other [*Chang et al.*, 2004], resembling interactions of particles at kinetic level, validating the analogy to the particle VDFs [*Leubner and Vörös*, 2005b]. In fact, the interactions between coherent MHD structures in simulations lead to kappa distributions [*Chang et al.*, 2004]. Laboratory experiments on turbulent flows exhibiting long-range correlations show that a model which maximizes the nonextensive entropy function to reconstruct the spatial distribution of an averaged vorticity field describes the vorticity PDFs rather well [*Jung et al.*, 2004]. We are not in a position to describe quantitatively the solar wind as a multiscale out-of-equilibrium system with long-range correlations in terms of the nonextensive statistical physics. Such theory is still in its infancy [*Pavlos et al.*, 2015]. Nevertheless, there exist long-range correlations in the solar wind which are associated with turbulence interactions or with the

largest scales of speed fluctuations. The correlation length associated with solar wind turbulence is about 0.015 AU, while the correlation length of large-scale velocity fluctuations is roughly 0.25 AU [*Podesta et al.*, 2008]. Simple simulations of statistical distributions demonstrate the formation of kappa-like distributions from Gaussian distributions, when interaction terms and long-range correlations are included [*Leitner et al.*, 2011b]. We expect that the long-tailed PDFs or the change of the κ parameter in the solar wind also reflects the occurrence of processes exhibiting long-range correlations in the one-point unfiltered data sets. Therefore, the observed multiscale kappa functions might also be connected with the nonextensive statistical description comprising nonlocal interactions. Admittedly, the parameters which describe the generalized polytropic law associated with kappa VDFs (n, T, κ) [*Livadiotis*, 2015] should have a different meaning for multiscale PDFs.

The length of the data sets is critical for reaching statistical convergence in parameter estimations. In fact, careful examination of the radial velocity and radial magnetic field statistics in the solar wind has shown that $10^6 - 10^7$ data points are required for robust estimation of the third-order moments associated with skewed PDFs [*Podesta et al.*, 2009]. In other studies of third-order moment estimations, based on the Elsässer variables, the number of data points was a few thousands only [*Sorriso-Valvo et al.*, 2007]. However, it was argued by *Sorriso-Valvo et al.* [2010] that turbulence in the fast and slow streams has different properties; therefore, merging data into longer data sets to reach statistical convergence can be misleading. PDFs corresponding to magnetic field and speed fluctuations during the declining phase of the solar cycle 23 in 2003 were analyzed by *Burlaga and Viñas* [2004]. They considered 275 days in their statistical study, which included multiple corotating streams, corotating interaction regions, discontinuities, and turbulence. Nevertheless, the authors found that the multiscale fluctuations can be well fitted by the nonextensive model PDFs [*Burlaga and Viñas*, 2004].

As one can see from the above studies, long data intervals are needed for the robust estimation of statistical parameters associated with multiscale structures and turbulence. On the other hand, the inclusion of structures, boundaries, solar ejecta, compressional regions, and turbulence, occurring during long time intervals, would most certainly result in nonunique combinations of (n, T, κ). This would preclude the connection of model kappa PDFs with nonextensive statistics or particle VDFs. There is a clear need for a better understanding of the meaning of kappa PDFs over the larger scales which contain mixtures of different plasmas.

2.3. Parametric PDFs for the Magnetic Field

We consider four types of parametric distribution functions which correspond to additive, multiplicative, nonextensive statistical processes, and their combinations.

The symmetric Gaussian (normal) distribution P_n appears as a result of the additive central limit theorem: the sum of identically distributed independent random variables (each having an expected value μ and variance σ^2) is normally distributed:

$$P_n(x, \mu, \sigma) = \frac{1}{\sigma\sqrt{\pi}} \exp\left[-\frac{(x-\mu)^2}{\sigma^2}\right], \quad -\infty < x < \infty. \tag{1}$$

It has already been found that PDFs corresponding to the time-delayed differences $\delta(X(t,\tau)) = X(t+\tau) - X(t)$, calculated from solar wind time series $X(t)$, do not follow the normal distribution P_n over the small time scales τ [*Marsch and Tu*, 1997; *Sorriso-Valvo et al.*, 1999; *Burlaga and Viñas*, 2004]. This is the time scale of turbulence, coherent structures, and interaction regions, spanning from hours down to seconds. Due to correlations and nonlinear interactions, the small-scale PDFs are peaked and skewed and exhibit fat tails (the largest fluctuations occur more frequently than for normally distributed random fluctuations). However, random fluctuations over longer time scales τ (from hours to days) exhibit Gaussian distribution due to the loss of correlations.

The skewed lognormal distribution P_{Ln} appears as a result of multiplicative central limit theorem [*Crow and Shimizu*, 1988] and reads as follows:

$$P_{Ln}(x, \mu, \sigma) = \frac{1}{x}\frac{1}{\sigma\sqrt{\pi}} \exp\left[-\frac{(\log x - \mu)^2}{\sigma^2}\right], \quad 0 < x < \infty. \tag{2}$$

Here μ is a scale parameter while σ represents a shape parameter.

When no time-delayed differentiation is applied, the magnetic field, density, and proton temperature statistics exhibit skewed PDFs which can be approximately modeled through the lognormal distribution [*Burlaga and Lazarus*, 2000; *Bruno et al.*, 2004; *Dmitriev et al.*, 2009; *Veselovsky et al.*, 2010a, 2010b]. Since lognormal distributions are generated through multiplications of random variables, logarithmic-scale invariance in turbulence is often understood in terms of multiplicative cascades [*Castaign et al.*, 1990]. In the solar wind random multiplications beyond turbulence are also foreseen for random amplification/weakening of waves or for compressional effects increasing the values of proton density or magnetic field [*Dmitriev et al.*, 2009]. In fact, the lognormal model describes rather well the density and temperature fluctuations with the highest probabilities (within $\pm 2\sigma$) or the magnetic field statistics (roughly within $\pm 1.5\sigma$). However, the fat tails present in data distributions show again probabilities higher than the P_{Ln} model [*Dmitriev et al.*, 2009]. This is also valid for the histograms of derived quantities, e.g., for the histogram of the solar wind quasi-invariant (the inverse square of the Alfvén-Mach number), which correlates well with sunspot cycle [*Leitner et al.*, 2011a]. We also mention that instead of a single lognormal PDF, two or more different lognormal models are added to form a single skewed one to fit the fluctuation statistics associated with the jumps in magnetic field vector orientation and magnetic field intensity [*Bruno et al.*, 2004]. It is supposed that different P_{Ln} models might be associated with different components of MHD turbulence, such as uncompressive fluctuations of Alfvénic origin or compressive structures. Three component lognormal models can also be associated with the anisotropic magnetic field-aligned (slab) and field-perpendicular (quasi 2-D) populations of fluctuations complemented by convected compressive structures [*Bruno et al.*, 2004]. It is not known how many different lognormal PDFs were needed to model the solar wind data.

A superposition of random uncorrelated, normally or lognormally distributed processes can provide a composed skewed PDF with fat tails which can fit the observations reasonably well. However, turbulent space plasmas contain structures, long-range interactions, and correlations. Normal (or for particles the Maxwell-Boltzmann) distributions are associated with Boltzmann-Gibbs statistics describing systems with noninteracting or weakly interacting subsystems in thermal equilibrium. For stationary nonequilibrium systems the Boltzmann-Gibbs entropy was generalized and the so-called nonextensive entropy was introduced by *Tsallis et al.* [1998]. The nonextensive entropy introduces interactions between subsystems (e.g., particles) [*Leubner*, 2002], and its extremization under certain physically relevant constraints leads to kappa distribution [*Tsallis et al.*, 1998; *Livadiotis and McComas*, 2013]. A simple physical model based on the generalized Galton board clearly demonstrates the formation of fat-tailed kappa-like distributions from Gaussian distributions, when interaction terms and memory effects are switched on [*Leitner et al.*, 2011b]. The peaked, fat-tailed data distributions corresponding to turbulence in the solar wind are well modeled by the kappa distribution [*Leubner and Vörös*, 2005a, 2005b]:

$$P_\kappa(x,\mu,\sigma,\kappa) = \frac{1}{\sigma\sqrt{\kappa\pi}}\frac{\Gamma(\kappa)}{\Gamma(\kappa-1/2)}\left(1+\frac{(x-\mu)^2}{\sigma^2\kappa}\right)^{-\kappa}, \quad -\infty < x < \infty. \tag{3}$$

The nonextensive κ index represents a measure of correlations or memory in systems out of equilibrium, when $\kappa \ll \infty$.

Since the kappa distribution represents a symmetric distribution, the observed skewed distributions [*Burlaga and Lazarus*, 2000] or the turbulent energy transfer rate ϵ [*Podesta et al.*, 2009] cannot be modeled by P_κ. *Burlaga and Viñas* [2004] added a somewhat artificial cubic term to their version of P_κ which could be used then to fit the observed skewed PDFs. An alternative approach to deal with the skewed PDFs was formally based on the assumption that the κ-distributed correlated fluctuations can also be combined in a multiplicative manner leading to the log-kappa distributions [*Leitner et al.*, 2009]:

$$P_{L\kappa}(x,\mu,\sigma,\kappa) = \frac{1}{x}\frac{1}{\sigma\sqrt{\kappa\pi}}\frac{\Gamma(\kappa)}{\Gamma(\kappa-1/2)}\left(1+\frac{(\log x-\mu)^2}{\sigma^2\kappa}\right)^{-\kappa}, \quad 0 < x < \infty. \tag{4}$$

The normal, lognormal, kappa, and log-kappa distributions are compared to each other in Figure 1. The nice feature of these model PDFs is that for $\kappa \to \infty$, $P_\kappa \Rightarrow P_n$ (Figure 1a) and $P_{L\kappa} \Rightarrow P_{Ln}$ (Figure 1b). In other words, depending on the values of κ (we show P_κ and $P_{L\kappa}$ for $\kappa = 3, 10, 20$), the kappa and log-kappa distributions are capable to reproduce the PDF tails which are fatter than the normal or lognormal PDFs. Although other types of parametric PDFs [e.g., *Consolini et al.*, 2009] or their combinations could also work well, we provide evidence that the considered PDFs are sufficient to model substantial parts of the observed magnetic fluctuations in the variable solar wind in 2008.

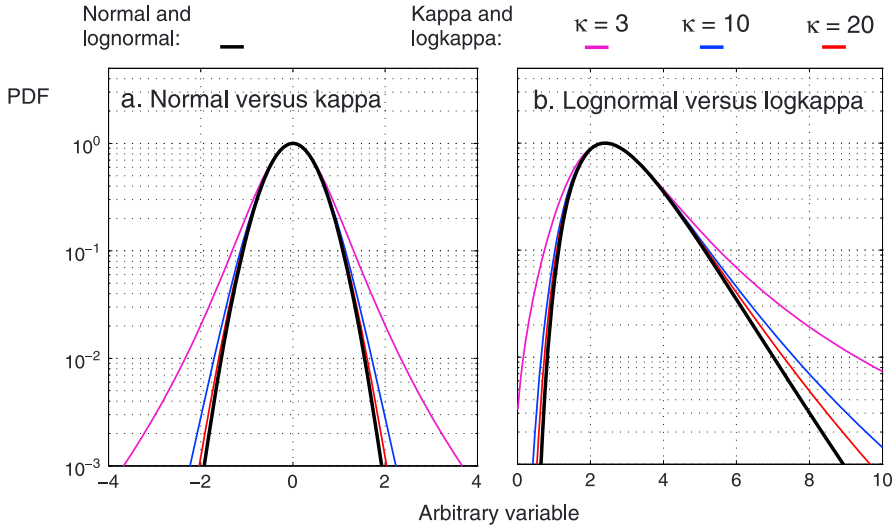

Figure 1. Comparison of theoretical probability density functions (PDFs) for different κ parameters. (a) Normal versus kappa model PDFs and (b) lognormal versus log-kappa model PDFs.

2.4. Fitting and Error Statistics

The Levenberg-Marquardt nonlinear least squares method [*Press et al.*, 1992] will be used to fit the parametric model PDFs to the histograms of the multiscale and time-delayed magnetic field fluctuations. The algorithm initially uses the gradient descent method to iteratively update the fitting parameters in large steps, and then it adaptively switches to Gauss-Newton method minimizing the sum of squares in smaller steps. Together with the fitted curves the 95% confidence intervals of the fits will be plotted. The error measure for the parameters is estimated as the square root of the diagonal of the parameter covariance matrix. The goodness of fit Q is calculated from the incomplete gamma function *gammq* as $Q = gammq(0.5\nu, 0.5\chi^2)$, where ν is the number of degrees of freedom and χ^2 is the "chi-square" parameter calculated from minimizing the sum of squares divided by the standard deviation [*Press et al.*, 1992]. The dependence of the model PDF parameters on the length of the time series will be calculated as well. Additionally, the skewness S (describing the asymmetry of PDFs) and its standard error will be estimated using a bootstrap method. The bootstrap is a Monte Carlo simulation method treating the original time series as a pseudopopulation from which new populations are obtained via random resampling [*Martinez and Martinez*, 2007].

3. Data Analysis

In this paper we use (NASA/GSFC's OMNIWeb) 1 min high-resolution plasma and magnetic data [*King and Papitashvili*, 2005, and references therein] near the solar cycle minimum in 2008. The subplots in Figures 2a–2c show the bulk speed (V), the magnetic field magnitude (B), and the dynamic pressure (P_{dyn}). The alternating fast-speed streams are interacting with the slower plasma leading to compressions in front of the streams [*Burlaga and Viñas*, 2004] and enhanced values of B and P_{dyn}. The trailing edge of the fast streams is characterized by lower values of B and P_{dyn}. The threshold $P_{dyn} = 3$ nPa, indicated by the red dashed horizontal line in Figure 2c, roughly separates the compression-dominated leading edges from the trailing edges of the streams. Figure 3 shows the scatterplots of B versus P_{dyn}, including two different streams (blue and black points for each) from the beginning of 2008. Both data sets (blue and black points) comprise a whole stream, i.e., leading edge and trailing edge data. Again, the red dashed line corresponding to the threshold $P_{dyn} = 3$ nPa separates the compressional leading edge from the trailing edge fluctuations. Any other stream interval in 2008 shows resemblance to the two examples in Figure 3. Since the compressions can produce lognormally distributed multiplications of the magnetic field [*Dmitriev et al.*, 2009] which are not present in the trailing edge regions of the streams, we may consider the possibility that the corresponding magnetic fluctuations are ruled by different statistical laws. To test this, we consider the magnetic fluctuation statistics for the whole year in 2008 and conditional statistics for the subsets of the data defined by $B(P_{dyn} > 3)$ nPa and by $B(P_{dyn} < 3)$ nPa. For the yearly statistics we consider the whole data set in 2008. For conditional statistics data corresponding to the short sudden transitions at the front of the leading edges of streams are discarded. Mixed data intervals

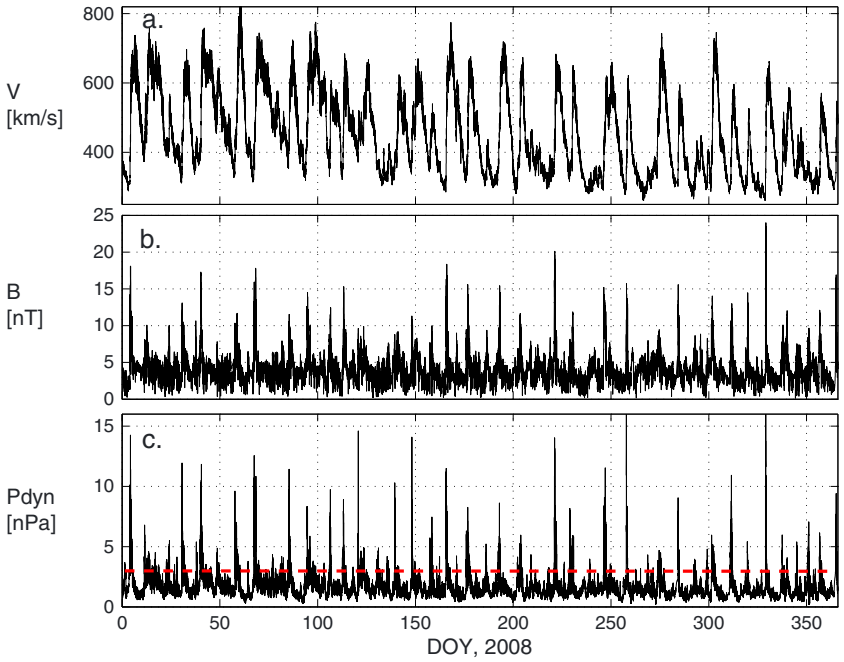

Figure 2. OMNI solar wind data near the solar cycle minimum in 2008. (a) Bulk speed V; (b) total magnetic field B; and (c) dynamical pressure P_{dyn}. The red dashed horizontal line indicates the threshold separating compressional data (P_{dyn} >3 nPa) at the leading edge of high-speed streams from the uncompressional data (P_{dyn} <3 nPa) at the trailing edge of high-speed streams.

with alternating short-duration large-amplitude pressure fluctuations, containing intervals with P_{dyn} below and over the 3 nT threshold, are also omitted. The compressional intervals represent roughly 5% and the trailing edge intervals 50% of the 527,040 data points in 2008.

3.1. Multiscale PDFs

Figures 4a1, 4b1, and 4c1 show the histograms corresponding to total magnetic field fluctuations B (blue points) and the parametric model PDF fits (P_{Ln}, $P_{L\kappa}$, and P_n) with confidence intervals. The maxima of the distributions are normalized to 1. Figures 4a2, 4b2, and 4c2 show the absolute values of residuals R, corresponding to the difference between data and PDF models. The histogram for the whole year in 2008 is shown in Figure 4a1. The fits and the black and red residuals in Figures 4a1 and 4a2, corresponding to

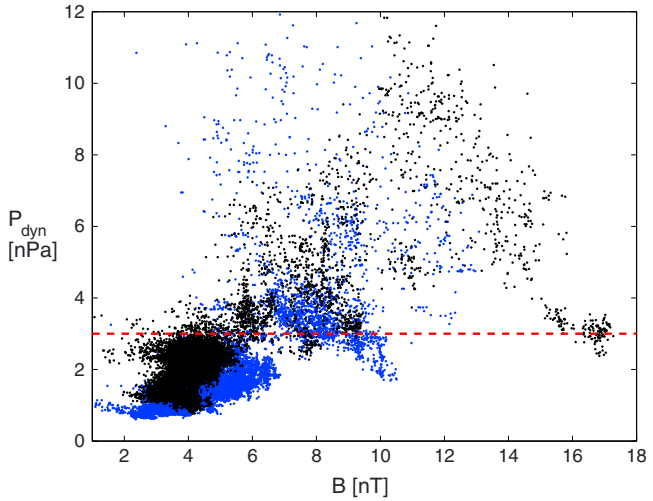

Figure 3. Scatterplot of magnetic field magnitude B versus dynamic pressure P_{dyn}. Two different high-speed streams are shown (blue and black points) from the beginning of 2008. The threshold P_{dyn} = 3 nPa is indicated by the red dashed line.

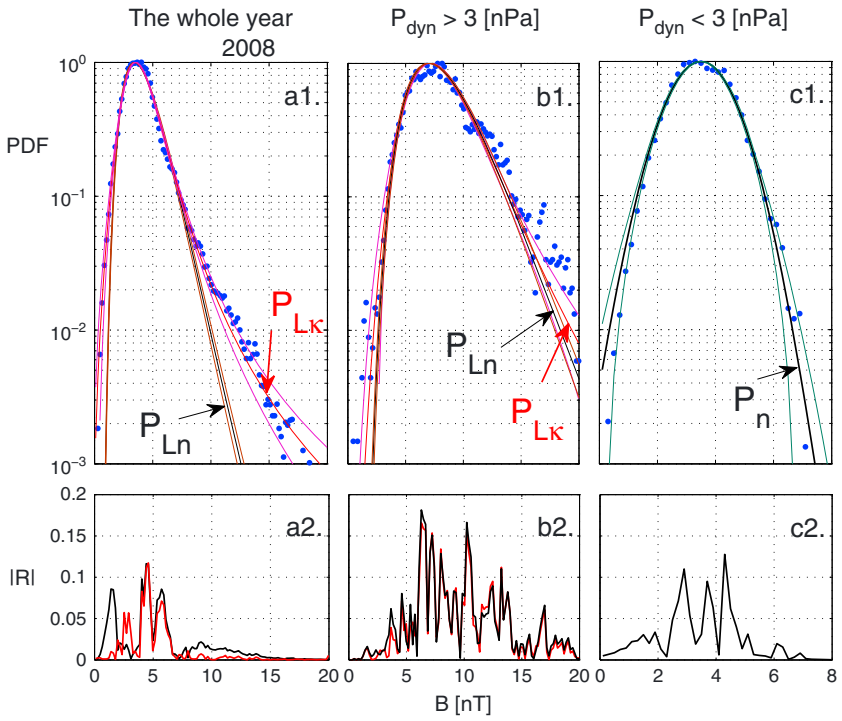

Figure 4. Comparison of the histograms of the total magnetic field fluctuations (B) with model PDFs and the absolute values of the residuals $|R|$. (a1, a2) Statistics for the whole year in 2008; (b1, b2) conditional statistics of the concatenated leading edge compressional intervals; and (c1, c2) conditional statistics of the concatenated trailing edge uncompressional intervals. Normal (P_n), lognormal (P_{Ln}), and log-kappa ($P_{L\kappa}$) model PDFs are shown with 95% confidence intervals.

P_{Ln} and $P_{L\kappa}$, respectively, indicate that the magnetic fluctuations near the maximum of PDF are described by both distributions equally well. This agrees well with the results of *Dmitriev et al.* [2009] that the fluctuations with the highest probabilities near the PDF maxima are lognormally distributed. Our analysis demonstrates, however, that the fat tails of the histogram are much better described by the log-kappa model. These results describe fluctuation statistics over long time intervals associated with multiple physical processes and mixtures of plasmas.

Let us consider now conditional statistics for the subsets of compressional ($B(P_{dyn} > 3)$ nPa) and trailing edge ($B(P_{dyn} < 3)$ nPa) data. These cases are shown in Figures 4b1, 4b2, 4c1, and 4c2, respectively. As one can see, the compressional magnetic fluctuations form a skewed distribution while the trailing edge fluctuations are symmetric and normally distributed. The tails of the histogram associated with compressional fluctuations are described slightly better by the log-kappa PDF than the lognormal PDF. From the conditional PDFs (Figures 4b1 and 4c1) it becomes clear how the unconditional PDF (Figure 4a1) associated with the yearly mixture of processes is formed. The normally distributed trailing edge data encompassing the fluctuations between 0 and 8 nT (Figure 4c1) make the main contribution to the central part of the yearly PDF (Figure 4a1). Within the range of 0–20 nT, the skewed parts of the yearly PDF or the fat tails (Figure 4a1) are formed by the compressional magnetic fluctuations (Figure 4b1). The $P_{L\kappa}$ model provides a better fit of the tails than the P_{Ln} model indicating that the compressive fluctuations are associated with multiplicative processes which additionally involve long-range correlations.

The dependence of parameters (κ, σ, μ) for the $P_{L\kappa}$ and P_n models on the length of the time series is shown in Figures 5a–5c. The horizontal axis indicates the increasing length of the time series (sample size) for which the PDF model parameters and their errors are estimated with the above described Levenberg-Marquardt algorithm. The color code corresponds to the unconditional data (blue), compressional (black), and trailing edge data (red). The data sets have different maximal lengths. The parameters are estimated for data intervals of increasing lengths until the maximal lengths are reached. In Figure 5d the goodness of fit parameter Q is shown. The PDF models are statistically rejected when $Q \to 0$, for example, $Q \ll 0.05$.

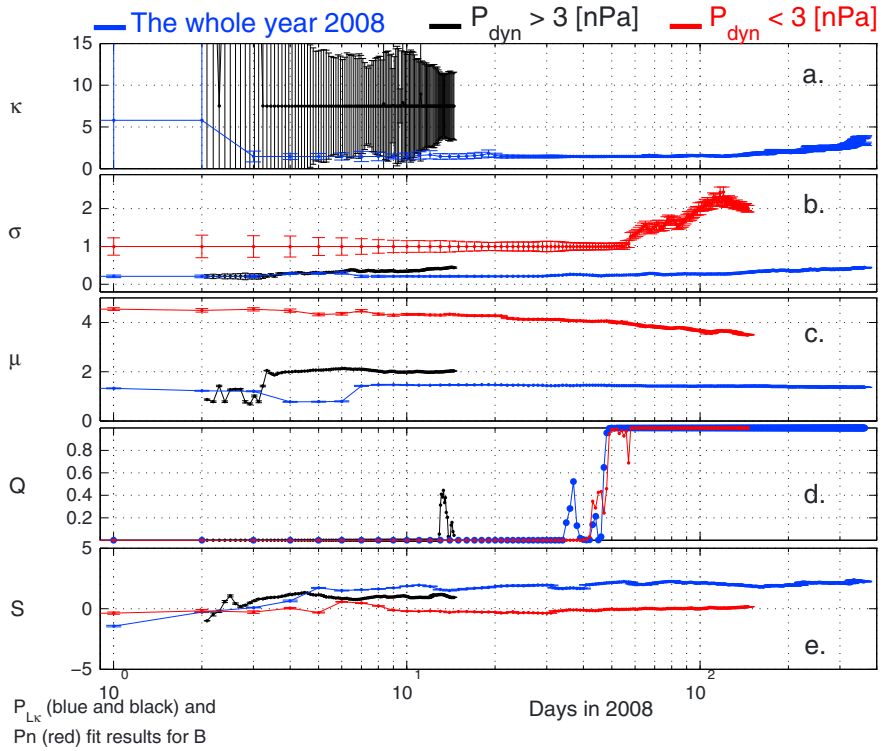

Figure 5. Dependence of fitting parameters on the data sample size for unconditional (blue) and conditional (black and red) total magnetic field (B) statistics, including the error bars. (a–c) Model PDF parameters κ, σ, and μ; (d) goodness of fit parameter Q; and (e) skewness S. The color code for conditional and unconditional statistics is indicated on the top of the figure; besides, the red color also corresponds to the P_n and the black and blue colors to the $P_{L\kappa}$ model fits. The parameters σ and μ are in nanotesla for P_n and dimensionless for $P_{L\kappa}$.

The PDF models are satisfactory when $Q > 0.05$ and the fitted parameters show stationarity. According to these criteria, the unconditional statistics calculated from the yearly data (blue curves) is well represented by the $P_{L\kappa}$ model when the lengths of data intervals are longer than 30–50 days, for which $Q > 0.05$. For the same intervals $\kappa \sim 2$ (blue curve in Figure 5a), indicating strong deviation of the log-kappa model from the lognormal model (Figure 1b). Roughly the same amount of trailing edge data (red curves in Figure 5) is required to reach statistical significance with the P_n model. However, when more than 40 day long intervals are considered, the parameters σ and μ show a quasi-stationary behavior. Since the P_n model is associated with conditional statistics, the required length of data intervals is longer than 40 days in the real time. The lengths of data intervals for the robust estimation of unconditional $P_{L\kappa}$ and trailing edge P_n statistics indicate that the underlying magnetic fluctuations might be associated with successive 27 day quasiperiodic recurrent streams. This is also valid for the multiscale compressional statistics (black curves in Figure 5). After more than 10 days of data Q becomes larger than 0.05 (Figure 5d). However, due to the $B(P_{dyn} > 3)$ nPa condition, the compressional data are collected from multiple streams during the whole year. Since the log-kappa and lognormal PDFs are rather similar (Figure 4b1), the κ parameter is large. At $Q > 0.05$ (Figure 5d) $\kappa = 8 \pm 4$ (Figure 5a). The relatively large errors (± 4) are caused by the small amount of compressional data ($\sim$24,000 data points).

The skewness (S) associated with the conditional and unconditional statistics is depicted in Figure 5e. The same color code is used as above. The error bars calculated from bootstrap are negligible. In accordance with the skewed PDFs (Figures 4a1 and 4b1), both the yearly and compressional data show positive skewness $S \sim 2$, while the skewness associated with normal PDF (Figure 4c1) is zero (Figure 5d).

The results of the model PDF fits together with S are shown in Table 1. The values of parameters correspond to the full lengths of data sets.

Table 1. PDF Model Fitting Statistics for the Multiscale Magnetic Fluctuations (B)[a]

Time Series	Skewness	PDF	μ	σ	κ
B	2.4 ± 0.1	P_{Ln}	1.36 ± 0.01	0.49 ± 0.01	
		$P_{L\kappa}$	1.36 ± 0.01	0.42 ± 0.05	3.5 ± 0.5
B ($P_{dyn} > 3$ nPa)	2 ± 0.1	P_{Ln}	2.06 ± 0.01	0.46 ± 0.01	
		$P_{L\kappa}$	2.06 ± 0.01	0.44 ± 0.01	8 ± 4
B ($P_{dyn} < 3$ nPa)	0.1 ± 0.1	P_n	3.5 ± 0.01	2 ± 0.15	

[a]The parameters σ and μ are in nanotesla for the P_n model.

3.2. Small-Scale PDFs

Figure 6 shows the histograms, PDF model fits, and the absolute residuals for the time-delayed differences $\delta B = B(t+\tau) - B(t)$, where $\tau = 10$ min. The same notation is used as in Figure 4. Since the histograms are rather symmetric, the P_κ and P_n model fits are compared. The residuals show (Figures 6a2, 6b2, and 6c2) that both models describe the central parts of the PDFs equally well. However, the kappa PDFs are better suited for the modeling of the fat tails. Despite the normally distributed multiscale fluctuations (Figure 4c1), the small-scale trailing edge PDF is peaked and long tailed (Figure 6c1). At the time scale of $\tau = 10$ min these fluctuations can be associated with inertial range turbulence. The same is true for the compressional fluctuations in Figure 6b1. However, the distribution is wider and large deviations have higher probabilities than in the trailing edge case. The unconditional yearly PDF in Figure 6a1 obviously contains a mixture of sudden jumps, trailing edge, and compressional fluctuations, all with different physical properties.

The dependence of parameters (κ, σ, μ) for the P_κ model on the length of the time series is shown in Figures 7a–7c. The goodness of fit parameter Q and the skewness S are shown in Figures 7d and 7e, respectively. The small-scale κ indices vary between 1.5 and 2 indicating strong correlations and fat tails at the given time scale τ. The parameter Q shows that the required length for the robust estimation of the model parameters is below 1 day for the conditional and 7–10 days for the yearly unconditional statistics. In comparison with

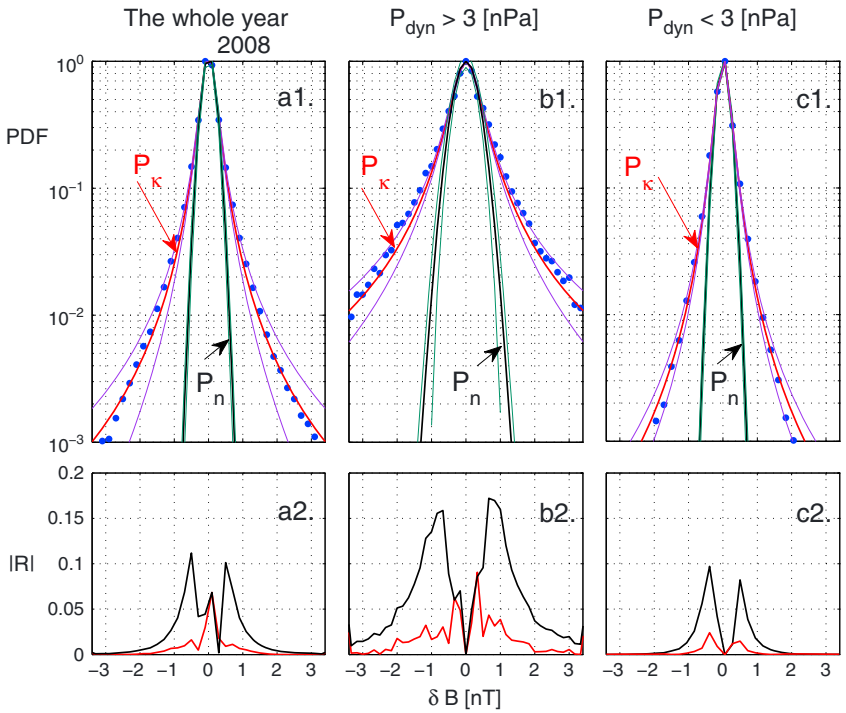

Figure 6. Comparison of the histograms of the time-delayed magnetic field fluctuations (δB) with model PDFs and the absolute values of the residuals $|R|$. (a1, a2) Statistics for the whole year in 2008; (b1, b2) conditional statistics of the concatenated leading edge compressional intervals; and (c1, c2) conditional statistics of the concatenated trailing edge uncompressional intervals. Normal (P_n) and kappa (P_κ) model PDFs are shown with 95% confidence intervals.

Table 2. PDF Model Fitting Statistics for the Time-Delayed Magnetic Fluctuations (δ)[a]

Time Series	Skewness	PDF	μ	σ	κ
δB	0.15 ± 0.1	P_n	0	0.032 ± 0.01	
		P_κ	0	0.03 ± 0.01	1.2 ± 0.05
δB ($P_{dyn} > 3$ nPa)	0.1 ± 0.1	P_n	0	0.2 ± 0.05	
		P_κ	0	0.18 ± 0.05	1.1 ± 0.2
δB ($P_{dyn} < 3$ nPa)	0 ± 0.05	P_n	0	0.04 ± 0.002	
	0 ± 0.05	P_κ	0	0.039 ± 0.002	1.58 ± 0.05

[a]The parameters σ and μ are in nanotesla for the P_n and the P_κ models.

the multiscale fluctuations, shorter data intervals are required for the robust estimation of model parameters over the small scales. This indicates that for the reliable estimation of the skewness, or perhaps the turbulent energy transfer rate ϵ, several hours or few days long data intervals might suffice. The results of the model PDF fits together with S are shown in Table 2. The values of parameters correspond to the full lengths of data sets.

A nonzero ϵ should be associated with skewed distributions; however, our PDFs are rather symmetric (Figure 6). *Podesta et al.* [2009] have pointed out that the third-order moments or the skewness represent signed moments subject to cancelation effects. Indeed, the skewness S calculated for the different δB data change sign in Figure 7e. Also, the error bars are of the same order as the mean values indicating the occurrence of strong nonstationarity effects. By increasing the sample size, the cancelation of successive positive and negative skewnesses can effectively lead to $S \sim 0$ hamstringing the calculation of the actual value of ϵ. In fact, S approaches zero for the largest sample sizes in Figure 7e. In hydrodynamics a skewness of zero would indicate no vortex stretching and no energy cascade in a turbulent flow [*Davidson*, 2004]. Positive or negative S could be associated with typical coherent structures such as sheets or tubes generated by vortex stretching or compression [*Davidson*, 2004]. In our case S simply changes sign when $\delta B = -B(t+\tau) + B(t)$ is considered

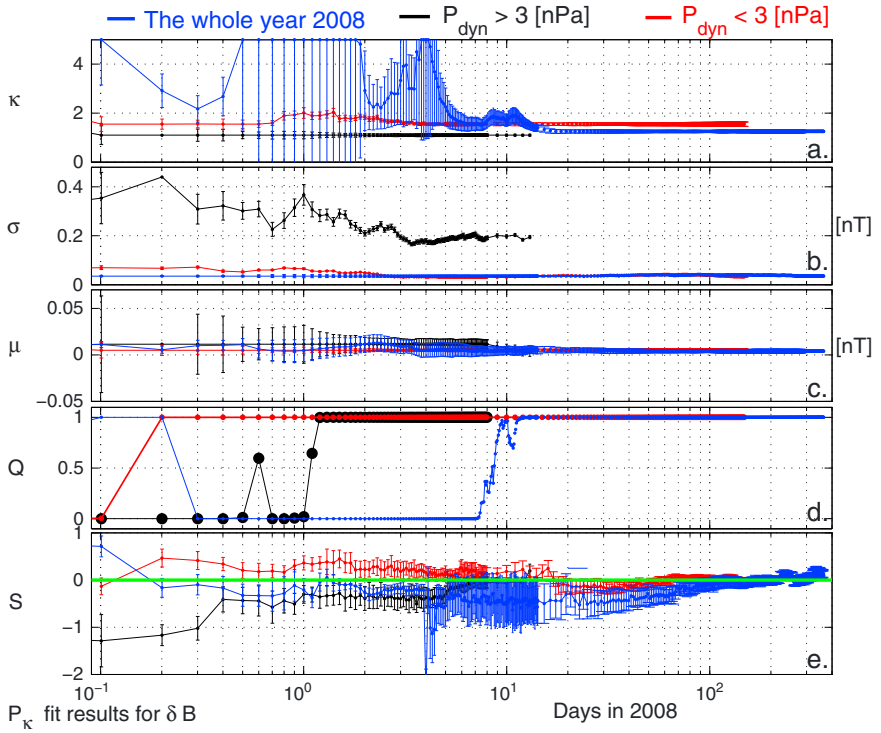

Figure 7. Dependence of fitting parameters on the data sample size for unconditional (blue) and conditional (black and red) time-delayed magnetic field (δB) statistics with error bars. (a–c) P_κ model parameters κ, σ, and μ; (d) goodness of fit parameter Q; and (e) skewness S. The color code for conditional and unconditional statistics is indicated on the top of the figure.

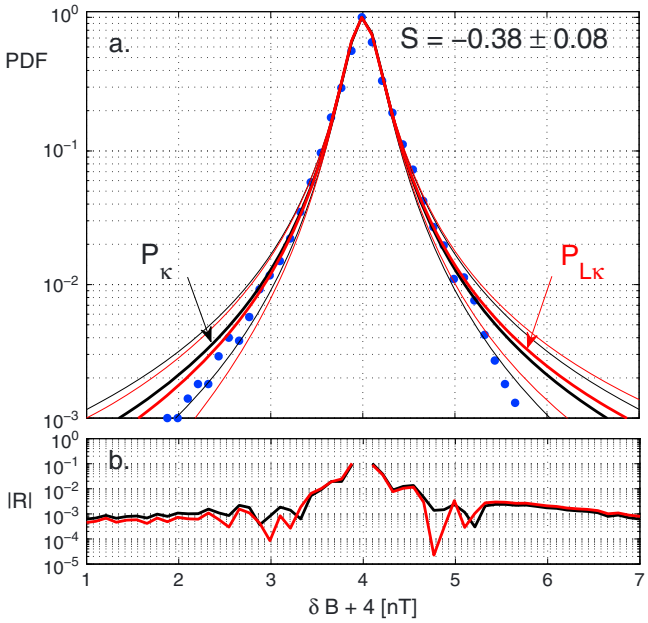

Figure 8. Comparison of the histograms of the time-delayed magnetic field fluctuations ($\delta B + 4$ nT) with (a) model PDFs and (b) the absolute values of the residuals $|R|$. Three subsets of trailing edge data in 2008 are concatenated, each with $S \sim -0.38$. The asymmetric $P_{L\kappa}$ model represents a slightly better fit of the fat tails than the symmetric P_κ model.

rather than $\delta B = B(t+\tau) - B(t)$. Therefore, one-point magnetic measurements of time-delayed differences do not allow the identification of sheet- or tube-like structures. When only the absolute values of S are considered separately for the trailing edge events, then the yearly average PDF becomes skewed at the given scale τ with $S = 0.25 \pm 0.1$.

A larger S can be obtained by considering subsets of the data. As an example, we selected three subsets of trailing edge data in 2008, each with $S \sim -0.38$ at $\tau = 10$ min. Bootstrap calculations for the concatenated data, consisting of 25,000 data points, give $S = -0.38 \pm 0.08$. Figure 8 shows the histogram of time-delayed magnetic fluctuations shifted by 4 nT to positive values. The shift does not affect the skewness; however, it allows a comparison of symmetric and skewed PDF models. Figure 8a shows the P_κ (symmetric, black line) and $P_{L\kappa}$ (asymmetric, red line) model fits. The absolute residuals in Figure 8b show that the central part of the histogram is fitted by the P_κ and $P_{L\kappa}$ models equally well. The tails of the histogram are described slightly better by the skewed $P_{L\kappa}$. Nevertheless, the fluctuations with the smallest probabilities deviate from the PDF models, possibly indicating finite size effects. Naturally, there exist several factors which can affect the statistical convergence of statistical parameters, such as S, ϵ, or the parameters of model PDFs. Our results show that beside the sample size the identification and separation of underlying physical processes are equally important.

4. Discussion and Conclusions

The main goal of this paper was to show that a limited number of parametric model PDFs can describe major parts of the magnetic fluctuations over multiple scales in the solar wind. The range of scales from minutes to several months predetermines the nature of physical processes occurring near a solar cycle minimum in the solar wind.

The large scales are dominated by a mixture of corotating streams, corotating interaction regions, solar ejecta, discontinuities, and turbulence [*Burlaga and Viñas*, 2004]. The multiscale statistics in this paper is based on the histograms of the 1 min total magnetic field fluctuations B obtained in 2008. Therefore, the large-scale processes and the fluctuations and turbulence over fluid scales contribute significantly to the multiscale statistics. This paper shows that the histogram associated with the multiscale mixture of physical processes is best described by the log-kappa $P_{L\kappa}$ model (Figure 4). Naturally, the κ parameter has a completely different meaning for the multiscale PDFs than for the almost instantaneous particle VDFs. Although the nonextensive interpretation of the κ index for the multiscale magnetic histograms is not straightforward, the log-kappa PDF model seems to be superior to the lognormal model even for longer time intervals encompassing

a solar cycle [*Leitner et al.*, 2011a]. This indicates that the κ index could have a reasonable interpretation over the multiscales as well. In order to further decipher the physics behind the multiscale log-kappa model, we used conditional PDFs, separating magnetic fluctuations according to the dynamic pressure. Conditional probability in space physics content has already been advocated by *Ukhorskiy et al.* [2004] to describe the multiscale features in solar wind-magnetosphere coupling. In our case, the pressure criteria separated fluctuations in space and time, roughly disengaging fluctuations at the leading edge of the fast streams where P_{dyn} >3 nPa, from the fluctuations at the trailing edge of the fast streams where P_{dyn} <3 nPa. It was demonstrated that the fluctuations of the magnetic field within the concatenated trailing edges are Gaussian distributed. It is not unexpected; the time-delayed differences $\delta(B(t,\tau)) = B(t+\tau) - B(t)$ for large τ also exhibit a normal distribution [*Sorriso-Valvo et al.*, 1999; *Burlaga and Viñas*, 2004]. Since for large enough τ the correlations in turbulence are lost, the multiscale trailing edge PDF appears to be the signature of uncorrelated magnetic fluctuations which are not affected by the small-scale turbulent cascades. Contrarily, the concatenated leading edge magnetic fluctuations associated with P_{dyn} >3 nPa are nonsymmetric. In this case the κ parameter in the skewed $P_{L\kappa}$ model is large ($\kappa = 8 \pm 4$, Table 1) and the log-kappa and lognormal PDF models are very close to each other. The "logarithmic" models associated with compressive fluctuations indicate the occurrence of multiplicative processes which has already been found by *Veselovsky et al.* [2010a, 2010b] and *Dmitriev et al.* [2009]. However, when the yearly PDF is considered, the mixture of normally distributed trailing edge and the lognormally distributed leading edge processes clearly forms a log-kappa distribution with $\kappa = 3.5 \pm 0.5$ (Figure 4), providing a better fit than the P_{Ln} model. Although the compressional data represent only ~5% of the total data set, the tails of the distribution are still determined by the most energetic contributions (in our case by the multiplicative compressional component) which occur more frequently than it would be expected for the outliers from a normal distribution. The other two parameters associated with P_{Ln} and $P_{L\kappa}$ models (μ and σ in Table 1) are similar. At this stage, however, it is impossible to interpret the κ index in terms of the nonextensive physics. The mixture of multiscale processes cannot be associated with a combination of (n, T, κ) parameters. Also, it is neither possible nor relevant to interpret the skewness associated with yearly or compressional multiscale fluctuations ($S = 2.4 \pm 0.1$ and $S = 2 \pm 0.1$, Table 1) as a quantity which could be related to energy transfer rate in a turbulent cascade. In this case S is simply associated with the asymmetry of PDFs. We offer here the interpretation that the multiscale κ index or S vary as the occurrence frequency of multiplicative processes, that is, the occurrences of stream/ejecta interaction regions and the associated fluctuations, change from year to year. This can influence the average properties of the solar wind, such as "the average amount of turbulence" or "the average rate of plasma heating" across a solar cycle. It has to be checked by further careful examination of the multiscale statistics. At the present time we have no models which could describe the multiscale variations of average properties of the solar wind plasma containing correlated and uncorrelated structures and a mixture of fluctuations.

The small-scale statistics is based on the histograms of the time-delayed differences $\delta(B(t,\tau)) = B(t+\tau) - B(t)$ obtained in 2008. The chosen time delay is $\tau = 10$ min; thus, the small scales are dominated by a mixture of turbulent fluctuations. The histograms at this scale in Figure 6 are best described by the kappa distributions with κ between 1.1 and 1.6 (Table 2). According to the nonextensive approach the kappa values are restricted to the interval $\kappa \in (1.5, \infty]$, simply because for $\kappa < 1.5$ the temperature is not determined for kappa VDFs [*Pierrard and Lazar*, 2010; *Livadiotis and McComas*, 2013]. The limiting value $\kappa = 1.5$ corresponds to the furthest state from equilibrium (or "antiequilibrium"), while $\kappa \to \infty$ corresponds to the equilibrium state associated with a Maxwellian VDF [*Livadiotis and McComas*, 2013]. It would be tempting to interpret the estimated values $\kappa \sim 1.5$ for δB PDFs as a signature of a thermodynamic antiequilibrium state. However, the histograms obtained from δB involve the yearly and concatenated mixtures of data and a unique antiequilibrium state would not account for the multiple physical processes occurring in 2008. We believe it is safer to say that the low values of κ index at the scale τ are associated with the structures repeatedly generated by turbulence introducing correlations to observed fluctuations. We mention that correlations in a generalized Galton board lead to peaked and fat-tailed kappa-like distributions, while in the absence of correlations Gaussian distributions are obtained [*Leitner et al.*, 2011b]. Figure 6 and the fitting results in Table 2 show that the κ and σ parameters are significantly different for the yearly and for each conditional PDFs. Although each histogram is peaked and fat tailed, the leading edge compressional data seem to be associated with a different type of turbulence than the trailing edge data. This might indicate that the multiscale, predominantly large-scale structures which are selected by the conditional statistics are affecting the small-scale turbulence.

The goodness of fit parameter Q depends on the data sample size. It is not surprising that for the robust estimation of multiscale model PDF parameters longer data sets are needed than for the small-scale model PDF parameters (Figures 5 and 7). The proper sample size ensuring a good fit, however, does not guarantee that the skewness S can be reliably calculated. S is a signed moment and therefore subject to cancelation effects. The consideration of longer data sets of δB containing alternating positive and negative S leads to $S \to 0$ which can be seen in Figure 7e. When only those subsets of data are considered for which the skewness is, for example, equal and negative, the skewed $P_{L\kappa}$ model describes the tails of the histogram slightly better than the symmetric P_{κ} model.

Finally, we mention that for the description of normal or peaked, fat-tailed, or skewed histograms the log-kappa and kappa PDF models might suffice. From these models the normal and lognormal distributions can be obtained by taking the limit $\kappa \to \infty$. Although other types of model PDFs or their combinations could also describe the peaked and skewed histograms well [*Consolini et al.*, 2009], the kappa and logarithmic kappa models allow to study the multiscale changes of histograms in a simple way. Anyhow, for a systematic study of the statistical variability in the solar wind, model PDFs have to be chosen. The kappa family of model PDFs seems to offer the desirable flexibility avoiding the unnecessary redundancy in modeling. Further studies are needed, however, to establish a firm connection between the nonextensive physics and the kappa distributions associated with turbulent or multiscale fluctuations. In order to estimate properly the skewness and the energy transfer rate, it would also be important to extend this analysis by considering conditional statistics for other physical quantities, including the Elsässer variables.

Acknowledgments
This work was supported by the Austrian Fond zur Förderung der wissenschaftlichen Forschung (projects P24740-N27) and by EU collaborative project STORM-313038. The OMNI data were obtained from the GSFC/SPDF OMNIWeb interface at http://omniweb.gsfc.nasa.gov.

Yuming Wang thanks Alexei Dmitriev and another reviewer for their assistance in evaluating this paper.

References

Alexandrova, O., C. H. K. Chen, L. Sorriso-Valvo, T. S. Horbury, and S. D. Bale (2013), Solar wind turbulence and the role of ion instabilities, *Space Sci. Rev.*, *178*, 101–139, doi:10.1007/s11214-013-0004-8.

Borovsky, J. E. (2008), Flux tube texture of the solar wind: Strands of the magnetic carpet at 1 AU?, *J. Geophys. Res.*, *113*, A08110, doi:10.1029/2007JA012684.

Bruno, R., and V. Carbone (2013), The solar wind as a turbulence laboratory, *Living Rev. Sol. Phys.*, *10*, 6813–6817.

Bruno, R., V. Carbone, L. Primavera, F. Malara, L. Sorriso-Valvo, B. Bavassano, and P. Veltri (2004), On the probability distribution function of small-scale interplanetary magnetic field fluctuations, *Ann. Geophys.*, *22*, 3751–3769.

Burlaga, L. F., and M. L. Goldstein (1984), Radial variations of large-scale magnetohydrodynamic fluctuations in the solar wind, *J. Geophys. Res.*, *89*, 6813–6817.

Burlaga, L. F., and A. J. Lazarus (2000), Lognormal distributions and spectra of solar wind plasma fluctuations: Wind 1995–1998, *J. Geophys. Res.*, *105*, 2357–2364.

Burlaga, L. F., and A. F. Viñas (2004), Multiscale structure of the magnetic field and speed at 1 AU during the declining phase of solar cycle 23 described by a generalized Tsallis probability distribution function, *J. Geophys. Res.*, *109*, A12107, doi:10.1029/2004JA010763.

Castaign, B., Y. Gagne, and E. J. Hopfinger (1990), Velocity probability density functions of high Reynolds number turbulence, *Physica D*, *46*, 177–200.

Chang, T., S. W. Y. Tam, and C. Wu (2004), Complexity induced anisotropic bimodal intermittent turbulence in space plasmas, *Phys. Plasmas*, *11*, 1287–1299.

Consolini, G., B. Bavassano, and P. De Michelis (2009), A probabilistic approach to heterogeneity in space plasmas: The case of magneic field intensity in solar wind, *Nonlinear Processes Geophys.*, *16*, 265–273.

Crow, E. L., and K. Shimizu (Eds.) (1988), *Log-Normal Distributions: Theory and Application, Stat. Textbooks Monogr.*, vol. 88, Marcel Dekker, New York.

Davidson, P. A. (2004), *Turbulence—An Introduction for Scientists and Engineers*, Oxford Univ. Press, Oxford, U. K.

Dmitriev, A. V., A. V. Suvorova, and I. S. Veselovsky (2009), Statistical characteristics of the heliospheric plasma and magnetic field at the Earth's orbit during four solar cycles 20–23, in *Handbook on Solar Wind: Effects, Dynamics and Interactions*, edited by H. E. Johannson, pp. 81–144, Nova Sci., New York.

Jung, S., B. D. Storey, J. Aubert, and H. L. Swinney (2004), Nonextensive statistical mechanics for rotating quasi-two-dimensional turbulence, *Physica D*, *193*(1–4), 252–264, doi:10.1016/j.physd.2004.01.035.

King, J. H., and N. E. Papitashvili (2005), Solar wind spatial scales in and comparisons of hourly Wind and ACE plasma and magnetic data, *J. Geophys. Res.*, *110*, A02104, doi:10.1029/2004JA010649.

Kolmogorov, A. N. (1941), Dissipation of energy in the locally isotropic turbulence [in Russian], *Dokl. Akad. Nauk SSSR*, *32*(1), 19–21.

Leitner, M., Z. Vörös, and M. P. Leubner (2009), Introducing log-kappa distributions for solar wind analysis, *J. Geophys. Res.*, *114*, A12104, doi:10.1029/2009JA014476.

Leitner, M., C. J. Farrugia, and Z. Vörös (2011a), Change of solar wind quasi-invariant in solar cycle 23—Analysis of PDFs, *J. Atmos. Sol. Terr. Phys.*, *73*, 290–293.

Leitner, M., M. P. Leubner, and Z. Vörös (2011b), Creating kappa-like distributions from a Galton board, *Physica A*, *390*, 1248–1257.

Leubner, M. P. (2002), A nonextensive entropy approach to kappa distributions, *Astrophys. Space Sci.*, *282*, 573–579.

Leubner, M. P. (2004), Fundamental issues on kappa-distributions in space plasmas and interplanetary proton distributions, *Phys. Plasmas*, *11*, 1308–1316.

Leubner, M. P., and Z. Vörös (2005a), A nonextensive entropy approach to solar wind intermittency, *Astrophys. J.*, *618*, 547–555.

Leubner, M. P., and Z. Vörös (2005b), A nonextensive entropy path to probability distributions in solar wind turbulence, *Nonlinear Processes Geophys.*, *12*, 171–180.

Livadiotis, G., and D. J. McComas (2010), Exploring transitions of space plasmas out of equilibrium, *Astrophys. J.*, *714*, 971–984.

Livadiotis, G., and D. J. McComas (2013), Understanding kappa distributions: A toolbox for space science and astrophysics, *Space Sci. Rev.*, *175*, 183–214.

Livadiotis, G. (2015), Statistical background and properties of kappa distributions in space plasmas, *J. Geophys. Res. Space Physics*, *120*, 1607–1619, doi:10.1002/2014JA020825.
Marsch, E. (2006), Kinetic physics of the solar corona and solar wind, *Living Rev. Sol. Phys.*, *3*, 1.
Marsch, E., and C. Y. Tu (1997), Intermittency, non-Gaussian statistics and fractal scaling of MHD fluctuations in the solar wind, *Nonlinear Processes Geophys.*, *4*, 101–124.
Martinez, W. L., and A. R. Martinez (2007), *Computational Statistics Handbook With Matlab*, Chapman and Hall, Boca Raton, Fla.
Pavlos, G. P., A. C. Iliopoulos, G. N. Zastenker, L. M. Zelenyi, L. P. Karakatsanis, M. O. Riazantseva, M. N. Xenakis, and E. G. Pavlos (2015), Tsallis non-extensive statistics and solar wind plasma complexity, *Physica A*, *422*, 113–135.
Pierrard, V., and M. Lazar (2010), Kappa distributions: Theory and applications in space plasmas, *Sol. Phys.*, *267*, 153–174.
Podesta, J. J., A. B. Gavlin, and C. J. Farrugia (2008), Correlation length of large-scale solar wind velocity fluctuations measured tangent to the Earth's orbit: First results from Stereo, *J. Geophys. Res.*, *113*, A09104, doi:10.1029/2007JA012865.
Podesta, J. J., M. A. Forman, C. W. Smith, D. C. Elton, Y. Malécot, and Y. Gagne (2009), Accurate estimation of third-order moments from turbulence measurements, *Nonlinear Processes Geophys.*, *16*, 99–110.
Politano, H., and A. Pouquet (1998), Von-Kármán-Howarth equation for magnetohydrodynamics and its consequences on third-order longitudinal structure and correlation functions, *Phys. Rev. E*, *57*, R21.
Press, W. H., S. A. Teukosky, W. T. Vetterling, and B. P. Flannery (1992), *Numerical Recipes in C*, 2nd ed., Cambridge Univ. Press, New York.
Scudder, J. D. (1992), On the causes of temperature change in inhomogeneous low-density astrophysical plasmas, *Astrophys. J.*, *398*, 299–318.
Smith, C. W., K. Hamilton, B. J. Vasquez, and R. J. Leamon (2006), Dependence of the dissipation range spectrum of interplanetary magnetic fluctuations on the rate of energy cascade, *Astrophys. J.*, *645*, L85–L88.
Sorriso-Valvo, L., V. Carbone, P. Veltri, G. Consolini, and R. Bruno (1999), Intermittency in the solar wind turbulence through probability distribution functions of fluctuations, *Geophys. Res. Lett.*, *26*, 1801–1804.
Sorriso-Valvo, L., R. Marino, V. Carbone, A. Noullez, F. Lepreti, P. Veltri, R. Bruno, B. Bavassano, and E. Pietropaolo (2007), Observation of inertial energy cascade in interplanetary space plasma, *Phys. Rev. Lett.*, *99*, 115001, doi:10.1103/PhysRevLett.99.115001.
Sorriso-Valvo, L., V. Carbone, R. Marino, A. Noullez, R. Bruno, and P. Veltri (2010), Reply, *Phys. Rev. Lett.*, *104*, 189002, doi:10.1103/PhysRevLett.104.189002.
Stawarz, J. E., C. W. Smith, B. J. Vasquez, M. A. Forman, and B. T. MacBride (2009), The turbulent cascade and proton heating in the solar wind at 1 AU, *Astrophys. J.*, *697*, 1119–1127.
Tsallis, C. (1988), Possible generalization of Boltzmann-Gibbs statistics, *J. Stat. Phys.*, *52*, 479–487, doi:10.1007/BF01016429.
Tsallis, C., R. S. Mendes, and A. R. Plastino (1998), The role of constraints within generalized nonextensive statistics, *Physica A*, *261*, 534–554.
Ukhorskiy, A. Y., M. I Sitnov, A. S. Sharma, and K. Papadopoulos (2004), Global and multi-scale features of solar wind-magnetosphere coupling: From modeling to forecasting, *Geophys. Res. Lett.*, *31*, L08802, doi:10.1029/2003GL018932.
Vasyliūnas, V. M. (1968), A survey of low-energy electrons in the evening sector of the magnetosphere with OGO1 and OGO3, *J. Geophys. Res.*, *73*, 2839–2884.
Veselovsky, I. S., A. V. Dmitriev, and A. V. Suvorova (2010a), Algebra and statistics of the solar wind, *Cosmic Res.*, *48*(2), 113–128, doi:10.1134/S0010952510020012.
Veselovsky, I. S., A. V. Dmitriev, and A. V. Suvorova (2010b), Lognormal, normal and other distributions produced by algebraic operations in the solar wind, in *Twelfth International Solar Wind Conference, AIP Conf. Proc.*, vol. 1216, edited by M. Maksimovic et al., pp. 152–155, Am. Inst. Phys., Melville.
Vörös, Z., M. P. Leubner, and W. Baumjohann (2006), Cross-scale coupling-induced intermittency near interplanetary shocks, *J. Geophys. Res.*, *111*, A02012, doi:10.1029/2005JA011479.
Vörös, Z., Y. L. Sasunov, V. S. Semenov, T. V. Zaqarashvili, R. Bruno, and M. Khodachenko (2014), Reconnection outflow generated turbulence in the solar wind, *Astrophys. J. Lett.*, *797*, L10, doi:10.1088/2041-8205/797/1/L10.
Zaqarashvili, T. V., Z. Vörös, and I. Zhelyazkov (2014a), Kelvin-Helmholtz instability of twisted magnetic flux tubes in the solar wind, *Astron. Astrophys.*, *561*, A62, doi:10.1051/0004-6361/201322808.
Zaqarashvili, T. V., Z. Vörös, Y. Narita, and R. Bruno (2014b), Twisted magnetic flux tubes in the solar wind, *Astrophys. J. Lett.*, *783*, L19, doi:10.1088/2041-8205/783/1/L19.